

In situ epitaxial MgB₂ thin films for superconducting electronics

X. H. Zeng,¹ A. V. Pogrebnnyakov,¹ A. Kotcharov,¹ J. E. Jones,¹ X. X. Xi,^{1,2,3,*} E. M. Lysczek,² J. M. Redwing,^{2,3} S. Y. Xu,¹ Qi Li,^{1,3} J. Lettieri,^{2,3} D. G. Schlom,^{2,3} W. Tian,⁴ X. Q. Pan,⁴ and Z. K. Liu^{2,3}

¹*Department of Physics, The Pennsylvania*

State University, University Park, PA 16802

²*Department of Materials Science and Engineering,*

The Pennsylvania State University, University Park, PA 16802

³*Materials Research Institute, The Pennsylvania*

State University, University Park, PA 16802

⁴*Department of Materials Science and Engineering,*

The University of Michigan, Ann Arbor, MI 48109

Abstract

A thin film technology compatible with multilayer device fabrication is critical for exploring the potential of the 39-K superconductor magnesium diboride for superconducting electronics. Using a Hybrid Physical-Chemical Vapor Deposition (HPCVD) process, it is shown that the high Mg vapor pressure necessary to keep the MgB₂ phase thermodynamically stable can be achieved for the *in situ* growth of MgB₂ thin films. The films grow epitaxially on (0001) sapphire and (0001) 4H-SiC substrates and show a bulk-like T_c of 39 K, a $J_c(4.2\text{K})$ of 1.2×10^7 A/cm² in zero field, and a $H_{c2}(0)$ of 29.2 T in parallel magnetic field. The surface is smooth with a root-mean-square roughness of 2.5 nm for MgB₂ films on SiC. This deposition method opens tremendous opportunities for superconducting electronics using MgB₂.

The newly-discovered 39-K superconductor magnesium diboride [1] holds great promises for superconducting electronics. However, success in fabricating MgB₂ Josephson junctions, the fundamental element of superconducting electronics, has been very limited due to the lack of an adequate thin film technology [2]. The main difficulty in depositing MgB₂ thin films is that a very high Mg vapor pressure is necessary for the thermodynamic stability of the MgB₂ phase at elevated temperatures [3]. The films deposited by the current technologies either have reduced T_c and poor crystallinity [4, 5, 6, 7, 8, 9, 10], or require *ex situ* annealing in Mg vapor [11, 12, 13]. The surfaces of these films are rough and non-stoichiometric [2, 12, 14], undesirable for Josephson junction devices. In this report, we show that epitaxial MgB₂ thin films can be deposited *in situ* by Hybrid Physical-Chemical Vapor Deposition (HPCVD), a novel combination of Physical Vapor Deposition (PVD) and Chemical Vapor Deposition (CVD). At a substrate temperature of around 750°C, the films grow epitaxially on (0001) sapphire and (0001) 4H-SiC substrates. They show bulk-like T_c , high critical current density J_c , and high upper critical field H_{c2} . The surfaces are smooth. The process is compatible with multilayer device fabrication and easy to scale up. These results mark the removal of a major road block towards a reliable MgB₂ Josephson junction technology.

MgB₂ has many properties that make it very attractive for superconducting electronics. Unlike cuprate high-temperature superconductors, MgB₂ seems to be a phonon-mediated superconductor [15] with a relatively long coherence length [16]. The grain boundaries in MgB₂ are not weak links [16, 17]. From the device perspective, MgB₂ is similar to Nb but with a higher T_c and larger energy gaps, even though two energy gaps exist [18, 19]. This will lead to higher speeds and higher operating temperatures than the Nb-based superconducting digital circuits. Moving the operating temperature from 5 K for Nb to 20 K for MgB₂ greatly reduces the cryogenic requirements, thus making superconducting electronics much more competitive.

For the deposition of MgB₂ thin films, a thermodynamic analysis predicted a growth window in the pressure-temperature phase diagram in which the MgB₂ phase is thermodynamically stable [3]. At temperatures necessary for epitaxial growth, the Mg vapor pressure in this growth window is very high for many vacuum deposition techniques. In practice, *in situ* growth of MgB₂ thin films has been demonstrated

below 320°C where the necessary Mg vapor pressure for phase stability is low [9, 10]. However, the temperature is too low for epitaxial growth, and the resultant films have lower T_c (34 K) and poor crystallinity. An alternative technique employs annealing of Mg-B or Mg-MgB₂ mixtures *in situ* in the growth chamber, at temperatures and duration such that severe Mg loss or MgB₂ decomposition does not occur [4, 5, 6, 7, 8, 20]. Films produced by such techniques also show lower T_c (34 K) and poor crystallinity [8]. By annealing B films *ex situ* in high Mg vapor pressure, temperatures as high as 900°C can be used [11, 12, 13]. The MgB₂ films thus produced show bulk T_c (39 K) and epitaxy [21, 22]. Unfortunately, this two-step *ex situ* annealing process is not desirable for multilayer device fabrication.

Our approach to meet the challenge of generating a high Mg vapor pressure is HPCVD. It is in principle similar to the Physical Vapor Transport (PVT) technique used to grow semiconductor single crystals [23]. In HPCVD, a standard vertical CVD quartz reactor is used and diborane, B₂H₆, is used as the boron precursor gas. Unlike conventional CVD which utilizes gaseous sources only, HPCVD uses heated bulk Mg (99.95%) as the Mg source. Before the deposition, a single crystal substrate is placed on the top surface of a SiC-coated graphite susceptor and bulk pieces of Mg are placed nearby. The reactor is then purged with purified N₂ gas and purified H₂ gas. The susceptor, along with the substrate and Mg pieces, are heated by an inductance heater to 730-760°C in the H₂ ambient. A mixture of 1000 ppm B₂H₆ in H₂ is then introduced into the reactor to initiate growth. The total pressure in the reactor is maintained at 100-700 Torr throughout the process. Due to the relatively high gas pressure and the flow pattern of the carrier gas in the reactor, the vapor from the heated pure Mg results in a high Mg vapor pressure near the substrate. When the B₂H₆ gas is not flowing through the reactor, there is no film deposition because of the low sticking coefficient of Mg at high temperatures [20]. Once the B₂H₆ gas begins to flow, a MgB₂ film starts to grow on the substrate. The deposition rate depends on the flow rate of B₂H₆ gas. For example, a flow rate of 25 sccm for the 1000 ppm B₂H₆ mixture results in a deposition rate of about 2-3 Å/s. After growth, the B₂H₆ gas is switched out of the reactor and the sample is cooled in the H₂ carrier gas to room temperature.

Films were deposited on (0001) sapphire and (0001) 4H-SiC substrates. They were

characterized for phase and structural information using four-circle x-ray diffraction with CuK_α radiation and a graphite monochromator. Fig. 1(A) shows a $\theta-2\theta$ scan of a MgB_2 film on a (0001) sapphire substrate. Beside the substrate peaks the only peaks observed arise from the (0001) planes of MgB_2 , indicating that a phase-pure MgB_2 film with c -axis orientation is obtained. The c lattice constant is 3.512 ± 0.005 Å, in agreement with the bulk value [15]. The full widths at half maximum (FWHM) of the 0002 peak were 0.47° and 1.6° in 2θ and ω , respectively. The in-plane orientation was probed with a ϕ -scan of the $10\bar{1}1$ MgB_2 reflection shown in Fig. 1(B). A six-fold symmetry characteristic of a (0001) oriented MgB_2 film with in-plane epitaxy is seen. The a lattice constant is 3.08 ± 0.02 Å, smaller than the bulk value of 3.14 Å [15]. The FWHM of this peak in ϕ is 1.65° . The plot reveals small peaks at $30^\circ \pm n \cdot 60^\circ$ (where n is an integer), indicating minimal amounts of 30° rotational twinning. The dominant in-plane epitaxial relationship is that the hexagonal MgB_2 lattice is rotated by 30° (i.e. $[10\bar{1}0] \text{ MgB}_2 \parallel [2\bar{1}\bar{1}0] \text{ Al}_2\text{O}_3$) to match the hexagonal lattice of sapphire, which has a lattice constant of 4.765 Å. X-ray diffraction of MgB_2 films on (0001) SiC substrates also revealed epitaxial growth with (0001) $\text{MgB}_2 \parallel$ (0001) SiC and $[2\bar{1}\bar{1}0] \text{ MgB}_2 \parallel [2\bar{1}\bar{1}0] \text{ SiC}$ and without 30° rotational twinning. The lattice parameters obtained are $c = 3.516 \pm 0.005$ Å and $a = 3.09 \pm 0.02$ Å, respectively. Due to the close lattice match between SiC ($a = 3.07$ Å for 4H-SiC) and MgB_2 , the hexagonal lattice of MgB_2 grows directly on top of the hexagonal lattice of SiC.

The same film described in Fig. 1 was studied by cross-section transmission electron microscopy (TEM). The measurement was performed in a JEOL 4000 EX microscope operated at 400 kV, providing a point-to-point resolution of 0.17 nm. Fig. 2(A) shows a low magnification bright-field TEM image. Fig. 2(B) and (C) are selected-area electron diffraction patterns taken from the film and the substrate with the incident electron beam along the same direction. Fig. 2(D) shows a high-resolution TEM image of the film/substrate interface. The results confirm the epitaxial growth of a c -axis oriented MgB_2 film on the sapphire substrate. The diffraction pattern in Fig. 2(B) is from the $[11\bar{2}0]$ zone axis of MgB_2 ; Fig. 2(C) is from the $[10\bar{1}0]$ zone axis of sapphire. This corroborates the x-ray diffraction results on the in-plane epitaxial relationship between the film and the sapphire substrate. Cross-section and plane-view TEM observations also show that the film consists of strongly faceted columns

with different heights, resulting from island growth. These columns have hexagonal shapes with very smooth top surfaces, and they have the same crystallographic orientations. An intermediate layer at the $\text{MgB}_2/\text{Al}_2\text{O}_3$ interface is seen in the high-resolution image. Fourier-transform studies and nano-sized probe electron diffraction reveal that the image characteristics of this layer result from a superposition of MgO regions with the epitaxially-grown MgB_2 . This intermediate layer is much thinner and simpler than that in the *ex situ* annealed epitaxial MgB_2 films, where layers of MgAl_2O_4 and MgO are observed [22].

It should be noted that the x-ray diffraction spectra are free of MgO peaks, which commonly appear in MgB_2 thin films grown by other techniques [4, 5, 8, 11, 13]. In cross-section TEM, MgO regions are seen only in a very thin layer near the $\text{MgB}_2/\text{Al}_2\text{O}_3$ interface, which may be the result of oxygen diffusion out of the substrate. We attribute the minimal oxygen contamination in the bulk of the MgB_2 films to the reducing ambient resulting from the use of hydrogen as the carrier gas in the process. When the susceptor and bulk Mg are heated to 750°C, H_2 effectively eliminates the oxide on the Mg surface and suppresses MgO formation during growth.

The superconducting and transport properties of the films were characterized by resistivity measurement using the standard four-point method. Fig. 3(A) shows a resistivity vs. temperature curve for a 2000 Å MgB_2 film on a sapphire substrate. The inset shows the details near the superconducting transition, and a zero-resistance T_c of 39.3 K is observed. The T_c value of 39 K is the same as that in the bulk materials, and has been repeatedly obtained in our MgB_2 films on sapphire and SiC substrates. The resistivity of the film is 10.5 $\mu\Omega\text{cm}$ at 300 K and 2.8 $\mu\Omega\text{cm}$ before the superconducting transition, giving a residual resistance ratio $RRR = R(300\text{K})/R(40\text{K})$ of 3.7. In our films with $T_c \sim 39$ K, we normally find RRR values of around 3.

The transport J_c for a 2900 Å thick MgB_2 films on a sapphire substrate is shown in Fig. 3(B) as a function of temperature and magnetic field. It was measured on a 30- μm wide bridge using a Quantum Design PPMS system with a 9-T superconducting magnet. The zero-field J_c is 1.2×10^7 A/cm² at 4.2 K, comparable to the best reported value in *ex situ* annealed films [13, 24]. The J_c drops under applied magnetic fields. When $H \perp$ film the rates at which J_c decreases is similar to that in *ex situ* annealed films with less oxygen contamination [13, 24], but faster than in *ex situ* annealed films

with substantial oxygen contamination [13]. This is consistent with the suggestion by Eom *et al.* that oxygen contamination in MgB₂ films provides pinning centers [13]. Because there is minimal oxygen contamination in our films as shown by the x-ray diffraction and TEM, the vortex pinning is weaker than in oxygen contaminated films. The suppression of J_c when $H \parallel$ film is much slower than for $H \perp$ film.

High-quality epitaxial MgB₂ thin films are valuable for basic studies of physical properties such as electronic anisotropy [25, 26, 27]. Fig. 3(C) shows the temperature dependence of the upper critical fields of a MgB₂ film on a SiC substrate when the magnetic field is applied perpendicular ($H_{c2}^{\perp}(T)$, solid triangles) and parallel ($H_{c2}^{\parallel}(T)$, open triangles) to the film plane (the (0001) plane). They are determined from the resistive transition by the intersection of a line tangent to the transition midpoint with a linear extrapolation of the normal state resistivity. A clear anisotropy between $H_{c2}^{\parallel}(T)$ and $H_{c2}^{\perp}(T)$ is observed. Because of the upward curvature near T_c , we calculate dH_{c2}/dT using the lower-temperature part of the data. Using the expression for the dirty-limit type-II superconductors, $H_{c2}(0) = 0.69T_c dH_{c2}/dT$, we find $H_{c2}^{\parallel}(0)$ and $H_{c2}^{\perp}(0)$ to be 29.2 T and 23.2 T, respectively, which yields an anisotropy ratio, $\eta \equiv H_{c2}^{\parallel}(0)/H_{c2}^{\perp}(0)$ of 1.26. Both the H_{c2} and η values are similar to those in *ex situ* annealed MgB₂ films [25].

The excellent epitaxy and superconducting properties of the MgB₂ films demonstrate that *in situ* growth of high-quality epitaxial MgB₂ films is possible as long as a sufficiently high Mg vapor pressure is produced. At 750°C, this pressure is about 10 mTorr in the thermodynamic growth window [3]. The HPCVD technique successfully achieves this value. The results also demonstrate the automatic composition control in the adsorption-controlled growth of films containing volatile species [28]. During the growth, the Mg:B ratio arriving at the substrate is likely above the 1:2 stoichiometry, but the extra Mg remains in the gas phase and the desired MgB₂ phase is always obtained. The deposition rate of MgB₂ is determined by the influx of diborane.

The *in situ* deposited MgB₂ films have mirror-like shiny surfaces. We have characterized the film surface by atomic force microscopy (AFM) (Nanoscope III). In Fig. 4, AFM images of MgB₂ films on (A) sapphire and (B) SiC substrates are shown. Clearly, films on the two substrates have very different morphologies. The surface of the film on SiC is smoother than that on sapphire substrate. When measured over

a large scan area, for example $10 \times 10 \mu\text{m}^2$, the root-mean-square (RMS) roughness for sapphire and SiC substrates are similar, ~ 4 nm. However, on a $1 \times 1 \mu\text{m}^2$ scale, the RMS roughness is ~ 4 nm for the film on sapphire and ~ 2.5 nm for the film on SiC. This is much smoother than any MgB_2 film surface published so far [12, 26]. The AFM images also show that the majority of the growth columns have dimensions larger than 100 nanometers, which is consistent with the TEM result.

The results presented here demonstrate that HPCVD is a viable film deposition technique for MgB_2 superconducting electronics. The epitaxial films produced by HPCVD have excellent superconducting properties and the small roughness of the film is promising for Josephson junctions. Furthermore, the *in situ* process can be readily scaled up to deposit over large substrate areas and offers the potential for multilayer heterostructure fabrication. As the technique is further refined and the film quality improved, emphasis can shift from MgB_2 film deposition to the fabrication of MgB_2 Josephson junctions and circuits. Finally, the availability of high-quality epitaxial thin films is anticipated to benefit a variety of fundamental studies of MgB_2 .

References and Notes

- * To whom correspondence should be addressed (at The Pennsylvania State University).
E-mail:xxx4@psu.edu
- [1] J. Nagamatsu, N. Nakagawa, T. Muranaka, Y. Zenitani, J. Akimitsu, *Nature* 410, 63 (2001).
 - [2] D. Mijatovic, A. Brinkman, I. Oomen, G. Rijnders, H. Hilgenkamp, *et al.*, *Appl. Phys. Lett.* 80, 2141 (2002).
 - [3] Z. K. Liu, D. G. Schlom, Q. Li, X. X. Xi, *Appl. Phys. Lett.* 78, 3678 (2001).
 - [4] D. H. A. Blank, H. Hilgenkamp, A. Brinkman, D. Mijatovic, G. Rijnders, *et al.*, *Appl. Phys. Lett.* 79 (2001).
 - [5] H. Christen, H. Zhai, C. Cantoni, M. Paranthaman, B. Sales, *et al.*, *Physica C* 353, 157 (2001).
 - [6] S. R. Shinde, S. B. Ogale, R. L. Greene, T. Venkatesan, P. C. Canfield, *et al.*, *Appl. Phys. Lett.* 79, 227 (2001).
 - [7] G. Grassano, W. Ramadan, V. Ferrando, E. Bellingeri, D. Marré, *et al.*, *Supercond. Sci. Techno.* 16, 742 (2001).
 - [8] X. H. Zeng, A. Sukiasyan, X. X. Xi, Y. F. Hu, E. Wertz, *et al.*, *Appl. Phys. Lett.* 79, 1840 (2001).
 - [9] K. Ueda, M. Naito, *Appl. Phys. Lett.* 79, 2046 (2001).
 - [10] W. Jo, J.-U. Huh, T. Ohnishi, A. F. Marshall, M. R. Beasley, *et al.*, *unpublished* (2002).
 - [11] W. N. Kang, H.-J. Kim, E.-M. Choi, C. U. Jung, S.-I. Lee, *Science* 292, 1521 (2001).
 - [12] H. Y. Zhai, H. M. Christen, L. Zhang, M. Paranthaman, C. Cantoni, *et al.*, *J. Mater. Res.* 16, 2759 (2001).
 - [13] C. B. Eom, M. K. Lee, J. H. Choi, L. Belenky, X. Song, *et al.*, *Nature* 411, 558 (2001).
 - [14] S. Y. Lee, J. H. Lee, J. H. Lee, J. S. Ryu, J. Lim, *et al.*, *Appl. Phys. Lett.* 79, 3299 (2002).
 - [15] S. L. Bud'ko, G. Lapertot, C. Petrovic, C. E. Cunningham, N. Anderson, *et al.*, *Phys. Rev. Lett.* 86, 1877 (2001).
 - [16] D. K. Finnemore, J. E. Ostenson, S. L. Bud'ko, G. Lapertot, P. C. Canfield, *Phys.*

- Rev. Lett.* 86, 2420 (2001).
- [17] D. C. Larbalestier, L. D. Cooley, M. O. Rikel, A. A. Polyanskii, J. Jiang, *et al.*, *Nature* 410, 186 (2001).
 - [18] S. Tsuda, T. Yokoya, T. Kiss, Y. Takano, K. Togano, *et al.*, *Phys. Rev. Lett.* 87, 177006 (2001).
 - [19] H. Schmidt, J. F. Zasadzinski, K. E. Gray, D. G. Hinks, *Phys. Rev. Lett.* 88, 127002 (2002).
 - [20] N. Newman, *private communication* .
 - [21] S. D. Bu, D. M. Kim, J. H. Choi, J. Giencke, S. Patnaik, *et al.*, *submitted to Appl. Phys. Lett.* .
 - [22] W. Tian, X. Q. Pan, S. D. Bu, D. M. Kim, J. H. Choi, *et al.*, *submitted to Appl. Phys. Lett.* .
 - [23] G. Kamler, J. Zachara, S. Podsiadlo, L. Adamowicz, W. Gebicki, *J. Crystal Growth* 212, 39 (2000).
 - [24] H.-J. Kim, W. N. Kang, E.-M. Choi, M.-S. Kim, K. H. P. Kim, *et al.*, *Phys. Rev. Lett.* 87, 087002 (2001).
 - [25] M. H. Jung, M. Jaime, A. H. Lacerda, G. S. Boebinger, W. N. Kang, *et al.*, *Chem. Phys. Lett.* 343, 447 (2001).
 - [26] C. Ferdeghini, V. Ferrando, G. Grassano, W. Ramadan, E. Bellingeri, *et al.*, *Supercond. Sci. Technol.* 14, 952 (2001).
 - [27] S. Patnaik, L. D. Cooley, A. Gurevich, A. A. Polyanskii, J. Jiang, *et al.*, *Supercond. Sci. Technol.* 14, 315 (2001).
 - [28] J. Y. Tsao, *Materials Fundamentals of Molecular Beam Epitaxy* (Academic Press, Boston) (1993).
 - [29] We gratefully acknowledge Arsen Soukiassian, Srinivasan Raghavan, and Kok-Keong Lew for their help in setting up the HPCVD system. This work is supported in part by ONR under grant Nos. N00014-00-1-0294 (XXX) and N0014-01-1-0006 (JMR), by NSF under grant Nos. DMR-9876266 and DMR-9972973 (QL), DMR-9875405 and DMR-9871177 (XQP), DMR-9983532 (ZKL), and by DOE through grant DE-FG02-97ER45638 (DGS).

FIGURE CAPTIONS

FIG. 1: X-ray diffraction spectra of a MgB_2 film on a (0001) sapphire substrate showing an epitaxial orientation relationship. (A) The $\theta - 2\theta$ scan showing a phase-pure c -axis oriented MgB_2 film. The spectrum is free from MgO peaks. (B) The ϕ -scan of the $10\bar{1}1$ MgB_2 reflection. The six-fold symmetry indicates a (0001)-oriented MgB_2 film with in-plane epitaxy. Weak peaks at $30^\circ \pm n 60^\circ$ indicate minimal amounts of 30° rotational twinning. The dominant epitaxial relationship is that the hexagonal MgB_2 lattice is rotated by 30° to match the hexagonal lattice of sapphire. For (0001) 4H-SiC substrate, MgB_2 films grow epitaxially with c -axis orientation and the hexagonal lattice of MgB_2 grows directly on top of the hexagonal lattice of SiC.

FIG. 2: Microstructure and interfacial atomic structure of the same film described in Fig. 1 studied by cross-sectional TEM. (A) A low magnification bright-field TEM image. (B) Selected-area electron diffraction (SAED) pattern from the MgB_2 film showing a $[11\bar{2}0]$ zone-axis diffraction pattern. (C) An SAED pattern from the sapphire substrate with the incident electron beam along the same direction as in (B), showing a $[10\bar{1}0]$ zone-axis diffraction pattern. The results confirm the in-plane epitaxial relationship described in Fig. 1. (D) A high-resolution TEM image of the film/substrate interface showing an intermediate layer. The image characteristics of the intermediate layer results from a superposition of epitaxial MgB_2 and regions of MgO .

FIG. 3: Superconducting and transport properties of MgB_2 thin films. (A) Resistivity vs. temperature for a 2000 Å thick MgB_2 film on a sapphire substrate. A zero-resistance T_c of 39.3 K is clearly shown in the inset. (B) Critical current density J_c of a 2900 Å thick MgB_2 film on a sapphire substrate as a function of magnetic field at different temperatures. The 4.2 K data include both $H \parallel$ film and $H \perp$ film, and only $H \perp$ film data are shown for other temperature. (C) Upper critical fields H_{c2} of a MgB_2 film on a SiC substrate when the magnetic field is applied perpendicular (solid triangles) and parallel (open triangles) to the film plane. We find $H_{c2}^{\parallel}(0) \approx 29.2$ T, $H_{c2}^{\perp}(0) \approx 23.2$ T, and the anisotropy ratio $\eta = 1.26$.

FIG. 4: AFM images of epitaxial MgB_2 films on (A) a sapphire and (B) a SiC substrates. The vertical scale is 200 nm/div. The two films have very different surface morphologies, and the film on SiC is smoother than that on the sapphire substrate. The RMS roughness is ~ 4 nm for the film on sapphire and ~ 2.5 nm for the film on SiC. The AFM images also show that the majority of the growth columns have dimensions larger than 100 nanometers.

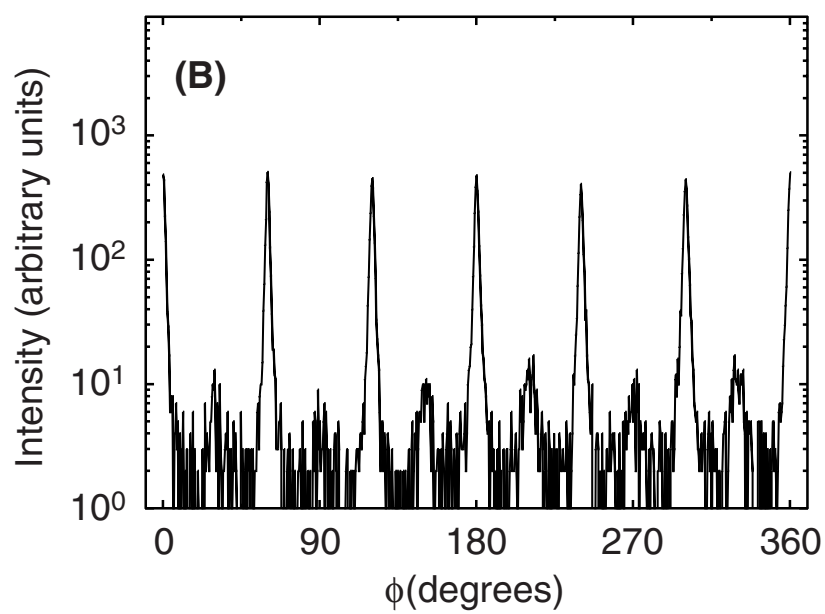
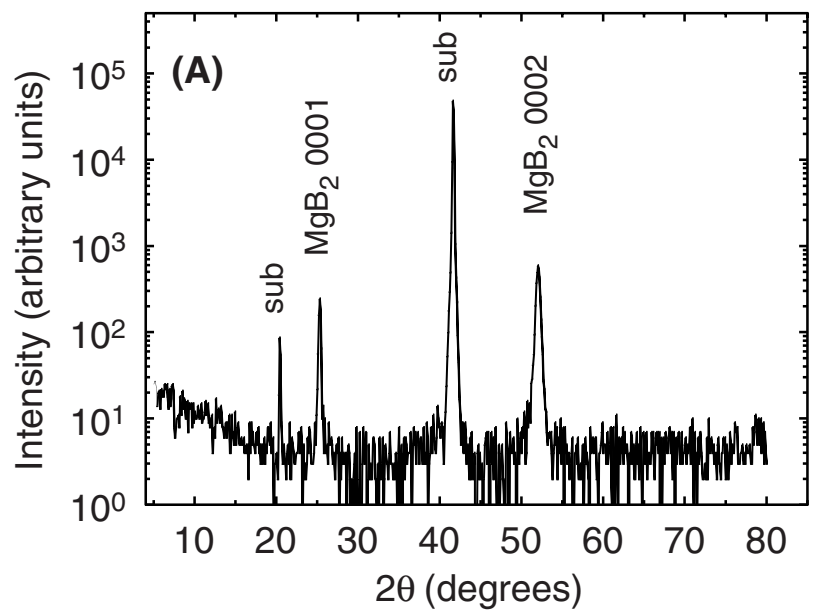


Figure 1 of 4
Zeng et al.

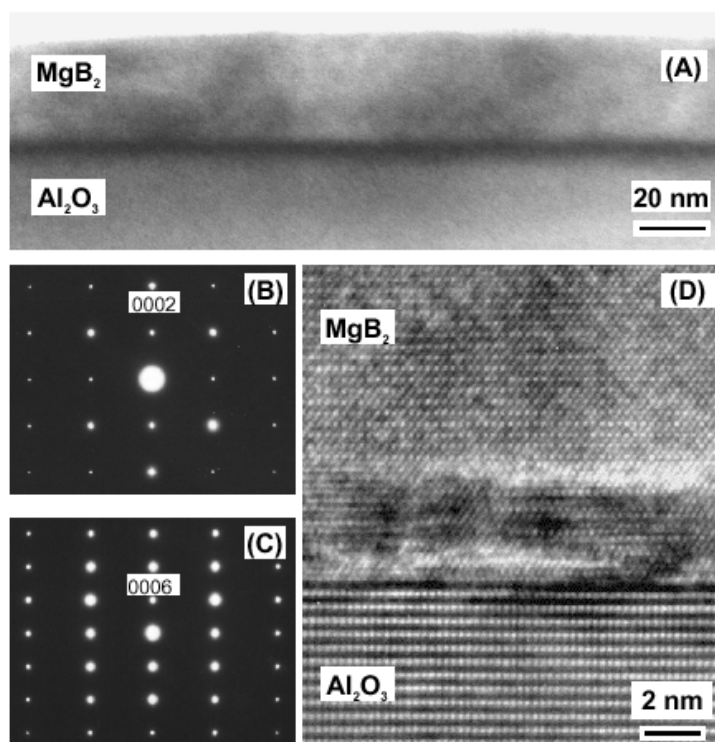


Figure 2 of 4
Zeng et al.

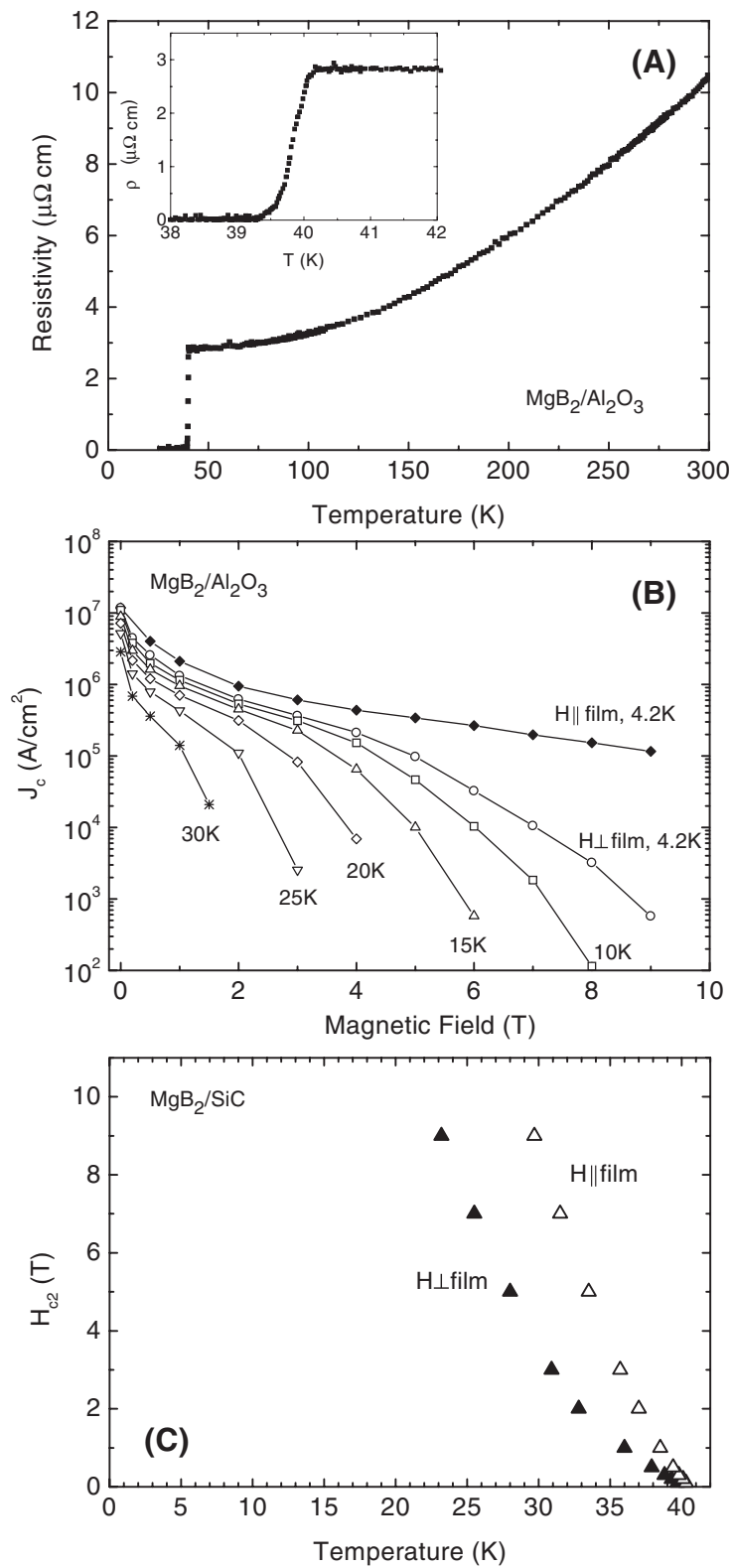


Figure 3 of 4
Zeng et al.

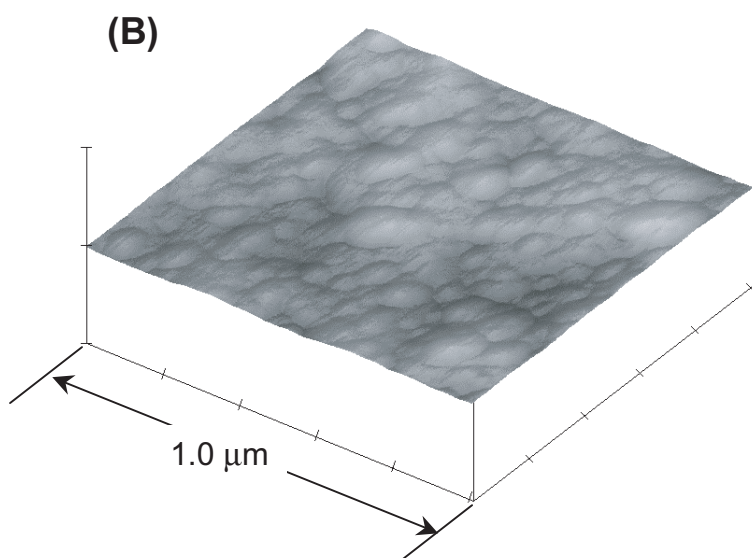
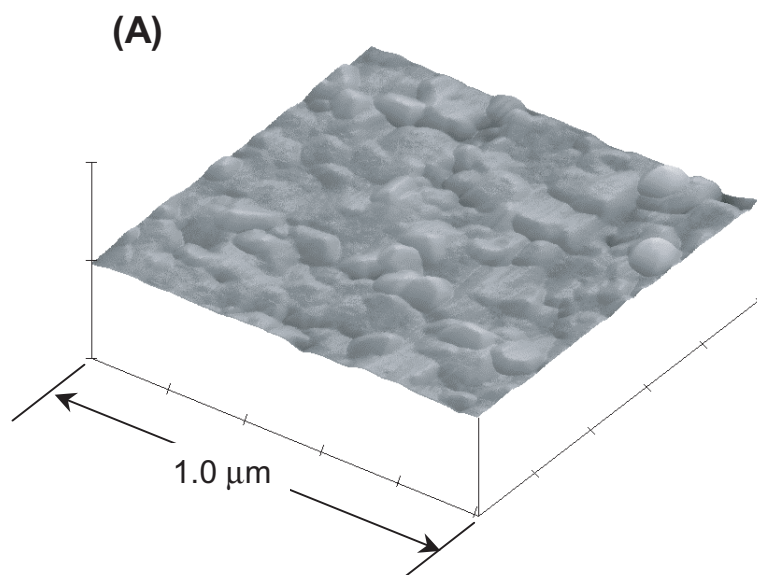


Figure 4 of 4
Zeng et al.